

Characterisation of thermo-mechanical properties of MgO–Al₂O₃–SiO₂ glass ceramic with different heat treatment temperatures

Z. Shamsudin · A. Hodzic · C. Soutis ·
R. J. Hand · S. A. Hayes · I. P. Bond

Received: 29 November 2010 / Accepted: 5 April 2011 / Published online: 4 May 2011
© Springer Science+Business Media, LLC 2011

Abstract The effects of heat treatment temperature on crystallisation behaviour, precipitated phases and thermo-mechanical properties of some MgO–Al₂O₃–SiO₂ (MAS) glass-ceramics were investigated. Crystallisation behaviour of MgO–Al₂O₃–SiO₂ glasses in the presence of TiO₂ as a nucleation agent was studied. The crystalline phases present in the heat treated samples were identified by X-ray diffraction (XRD). It was observed from XRD studies that magnesium aluminium titanate initially precipitated and when the heat treatment temperature was increased to 1140 °C, depending on the thermal history, either magnesium silicate, aluminium titanate and quartz or magnesium aluminium titanate, magnesium aluminate and quartz were precipitated. SEM observation revealed that the heat treatment led to phase separation of droplet-shaped crystals before the needle-shaped crystals formed at 1140 °C. The effect of annealing temperature on the density and mechanical properties of these glass-ceramic were characterised by nanoindentation and the results revealed a significant increase in hardness of the fully crystallised system.

Introduction

Recently MgO–Al₂O₃–SiO₂ glass-ceramics have been considered as matrix materials in the fabrication of ceramic matrix composites [1–4] for high-temperature composite applications. This system has been reported to have good materials properties such as high-Young's modulus and low thermal expansion coefficient [5–7], and increased hardness compared to the conventionally used E-glass [8, 9]. The distinctive properties of glass-ceramic systems arise from the formation of a major crystalline phase, tailored by suitable selection of its constituents and their stoichiometric proportions [10, 11]. Composition, nucleating agents and heat treatment process all influence the crystalline phases formed [12]. The strength of MgO–Al₂O₃–SiO₂ glass-ceramic depends on whether cordierite phase can develop as the major crystal phase. Cordierite glass-ceramics can possess strengths of up to ~250 MPa above 1200°C temperature of heat treatment. Cordierite glass-ceramics with very low thermal expansion coefficients can be produced in the MgO–Al₂O₃–SiO₂ system [13]. Although a number of studies have been reported aimed specifically at examining the relationship between nucleation and crystallisation in MAS glass-ceramic system, a literature survey revealed that not much work on mechanical properties, especially on the Young's modulus has been reported as of date.

Here the authors consider the production of MAS-fibres for the production of novel, high strength and composite materials. Relatively little work has been done concerning the fabrication of glass-ceramic fibres, even though such fibres potentially offer improved performance as compared to conventional glass reinforcing fibres. Ashbee [14] reported on the extrusion of SiO₂–Li₂O–ZnO glass-ceramics system using the extrusion method, and established a methodology followed by a number of researchers

Z. Shamsudin (✉) · A. Hodzic (✉) · C. Soutis
Department of Mechanical Engineering, The University
of Sheffield, Sheffield S1 3JD, United Kingdom
e-mail: meq08zs@sheffield.ac.uk

A. Hodzic
e-mail: a.hodzic@sheffield.ac.uk

R. J. Hand · S. A. Hayes
Department of Materials Science and Engineering,
The University of Sheffield, Sheffield S1 3JD, United Kingdom

I. P. Bond
Department of Aerospace Engineering, The University
of Bristol, Bristol BS8 1TR, United Kingdom

using different glass-ceramic systems [15, 16]. Onishi et al. [15] prepared glass performs to produce various $\text{BiO-PbO-SrO-CaO-CuO}$ glass-ceramics. These performs were heated to the softening point before successfully drawing into fibre with smooth surface and without observed porosity. Sakamoto and Yamamoto [16] used crystallised $\text{LiO}_2\text{-Al}_2\text{O}_3\text{-SiO}_2$ (LAS) preforms to study the drawing formability. The LAS glass-ceramic capillaries drawn from the crystallised perform show a low thermal expansion coefficient and excellent mechanical properties when converted into fibre form [5, 6]. Thus, the inclusion of glass-ceramic as a fibre in a composite material is expected to produce a significant improvement in Young's modulus of a composite material when compared to the same composite produced from glass fibres. Previously, a number of researchers used glass-ceramic MAS systems in their studies as the matrix for composites combined with other materials such as SiC fibres and whiskers. Therefore, this material is considered as a potential replacement for conventional reinforcing glass fibres in high-temperature structural advanced composite applications. When designing engineering components, mechanical properties of materials are used to determine their suitability for specific applications [17, 18]; these properties are correlated to development of crystalline phases and the microstructure of the materials. To develop a good fibre accompanied with a desired microstructure and subsequent materials properties, it is therefore necessary to investigate and assess their thermo-mechanical properties. The development of outstanding thermo-mechanical properties is achieved through fine-grained microstructures [9]. The favourable effect of the nucleation agents upon the crystallisation process in the MAS system has been reported in the literature [19–21]. The addition of TiO_2 into the MAS system significantly enhanced the crystallisation process and the thermo-mechanical properties of the resulting material. This nucleating agent is soluble in molten glasses, however, during cooling or subsequently reheating, large numbers of submicroscopic particles are precipitated and utilised in the development of major crystal phases. Preferred nucleating agents for MAS glass-ceramics are TiO_2 or combination of TiO_2 and ZrO_2 [10]. According to Zdaniewski [19] TiO_2 causes glass separation and furthermore lead to crystallisation. Many researchers have produced good mechanical properties arising from addition of TiO_2 to the glass [5, 6, 19, 22, 23]. Shao et al. [5] used TiO_2 as a nucleating agent for MAS glass-ceramics; following heat treatment at 1100 °C for 2 h, they obtained a maximum elastic modulus of 137 GPa accompanied by a microhardness of 8.5 GPa. This study is focussed on investigating the effect of heat treatment on the thermo-mechanical properties of the MAS glass-ceramic system. Correlation between the thermo-mechanical properties and crystalline phases is supported

by microstructural analysis after the heat treatments at different temperatures.

Experimental

Preparation of glasses and thermal processing

The composition of the glass-ceramic investigated in this study is shown in Table 1. The system was prepared from reagent-grade chemicals, except for SiO_2 , where high quality silica glass-making sand was used. This composition was chosen because of its reported good mechanical properties [6]. Batches were weighed and placed in alumina crucibles. They were then calcined overnight before melting at 1600 °C for 3 h in a gas furnace. The glass melts were cast as a block onto preheated steel plate and annealed as outlined in Table 2, before slow cooling to room temperature. As Wange et al. [6] reported that the crystallisation sequence during heat treatment depends on the prior annealing schedule two different annealing schedules were studied here. Then, the glass specimens were either crushed for differential thermal analysis (DTA) or cut into bars for further investigation. Based on the thermal analysis results (see below for details) the glass was converted into a range of glass-ceramics by different two step heat treatments. In all cases the first heat treatment involved holding the sample at 720 °C for 3 h. The second heat treatment involved a 2 h hold at temperatures between 850 and 1140 °C. In all cases the heating rate was 5 °C/min and the cooling rate was 1 °C/min.

Analytical characterisation

Glass-transition temperatures (T_g) and crystallisation exotherms (T_c) were measured using differential thermal analysis (DTA) on a Perkin Elmer Pyris ITGA-DTA 7 unit with a heating rate of 10 °C/min from room temperature to 1400 °C in air. The crystalline phases formed were identified using X-Ray diffraction (XRD) analysis of cross sectioned samples on a Siemens D500 X-ray diffractometer (Siemens D500) with $\text{Cu } K_\alpha$ radiation. The samples were scanned over the range 5–80° 2θ at a rate of 2° 2θ /min. For

Table 1 Glass composition

Oxide	Fraction (mol%)	Fraction (wt%)	Raw material	Purity (%)
SiO_2	57.3	51.4	SiO_2	99
Al_2O_3	19.0	28.9	$\text{Al}(\text{OH})_3$	>98
MgO	14.6	8.8	MgCO_3	>98
TiO_2	9.1	10.9	TiO_2	98

Table 2 Annealing schedules

Sample	Annealing temperature (°C)	Time (h)
A	700	1
	600	1
B	570	2

identification of the bulk phase, the samples were ground to remove any surface crystalline layers. The phases were identified by comparing the experimental X-ray diffraction patterns to standards compiled by the International Centre for Diffraction Data (ICDD).

Density measurement of both glass and glass-ceramics was carried out using the Archimedes technique with water as the immersion medium.

The morphologies of the crystalline phases developed on heat treatment of the glass samples were examined by scanning electron microscopy (SEM). The glass-ceramic samples were polished, etched with 2.5% HF solution for 30 s, coated with carbon and examined by an FEI Nova200 FEG-SEM instrument.

Nanohardness (H), and reduced elastic modulus (E_r) of the samples were measured on polished samples using a Triboscope (Hysitron Inc.) nanoindenter mounted on a Dimension 3100 (Veeco) nanoscope. The samples were prepared by successive grinding on a series of SiC papers and finally polishing with 6, 3, 1 and 0.25 μm diamond pastes. A load of 5 mN was applied with a Berkovich indenter, with 15 s upload, 15 s hold and 15 s download. Each sample was indented four times at five different locations under the same measuring conditions. The reduced modulus, E_r , was extracted from the stiffness, S , of the initial part of the unloading curve following the method of Oliver and Pharr [24]:

$$E_r = \frac{S}{\sqrt{A}} \frac{\sqrt{\pi}}{2} \quad (1)$$

where A is the projected contact area which was calculated from the contact depth, h_c . The nanohardness was obtained from the maximum load, P_{\max} , [25]:

$$H = \frac{P_{\max}}{A} \quad (2)$$

The reduced modulus is related to the properties of the sample, s , and the indenter, i , by

$$\frac{1}{E_r} = \frac{1 - v_s^2}{E_s} + \frac{1 - v_i^2}{E_i} \quad (3)$$

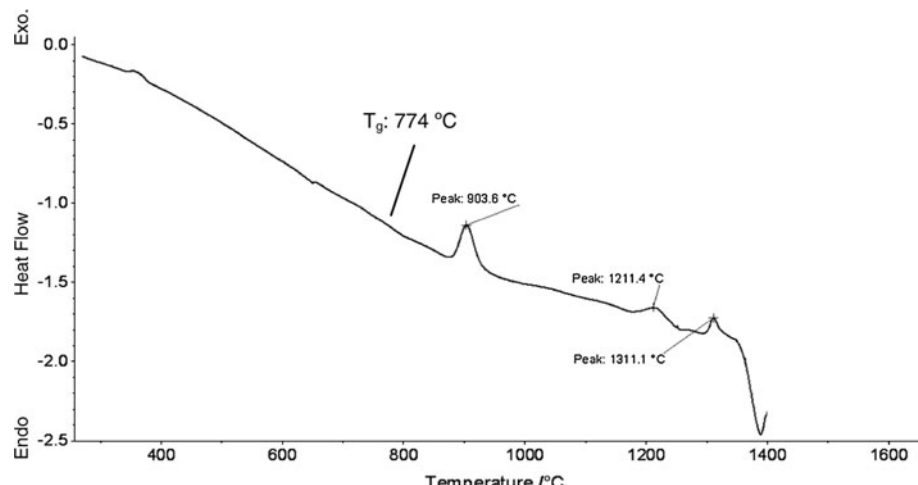
where E is Young's modulus and v is Poisson's ratio.

Results and discussion

DTA analysis

The DTA trace of the parent glass is given in Fig. 1. From Fig. 1, it is observed that samples exhibit three exothermic peaks which are denoted as phase I, phase II and phase III. The exothermic peak at 903.6 °C is relatively sharp whilst the others peaks are broad in comparison.

The samples changed colour on heat treatment (see Fig. 2). The brown colour seen in the as-annealed sample has previously been reported by Zdaniewski [19] and Wange et al. [6, 19] and is probably due to the presence of TiO_2 . However, Quyang et al. [23] reported that 9 wt% TiO_2 results in a light purple colour which then became opaque white as the heat treatment temperature was increased. It was also reported that varying the amount of TiO_2 in the composition produced visible changes in the appearance.

Fig. 1 DTA traces of the parent glass

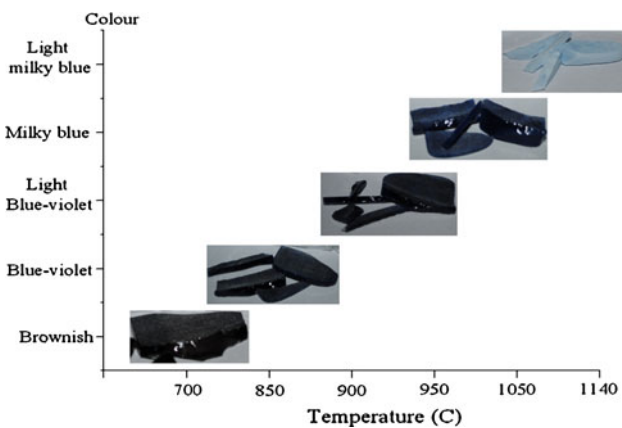


Fig. 2 Effect of heat treatment on the colour of $\text{MgO}-\text{Al}_2\text{O}_3-\text{SiO}_2$ glass

X-ray diffraction results

The complex crystalline phases in MAS system analysed in this study are abbreviated as T-magnesium aluminium titanate, M-magnesium aluminate, S-magnesium silicate, A-aluminium titanate and Q-quartz.

Sample A

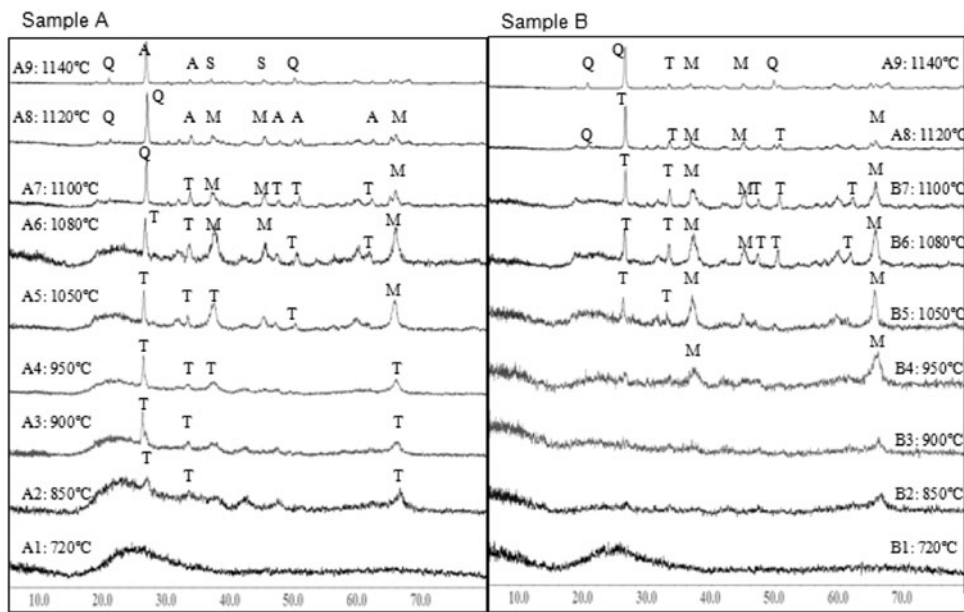
Figure 3 shows the XRD patterns of each glass after heat treatment. Sample A1 heat treated at 720 °C shows no indication of crystalline phases. The sample was XRD amorphous after the heat treatment of 3 h. Weak diffraction peaks are observed at 850 °C, indicating mainly glassy phase and a small amount of crystalline phase, namely magnesium aluminium titanate (T), $\text{MgAl}_2\text{Ti}_3\text{O}_{10}$ (JCPDF card: 5-450). Wange et al. [6] reported the formation of

quartz at 800 °C followed by the formation of magnesium aluminium titanate ($\text{Mg}_2\text{Al}_6\text{Ti}_7\text{O}_{25}$), which is similar to the results presented in this work. Quyang et al. [23] also reported that magnesium aluminium titanate appears after heat treatments at 850 and 900 °C.

Referring to the diffractogram of the sample A in Fig. 3, it was found that the predominant crystalline phase at 900 and 950 °C was magnesium aluminium titanate ($\text{MgAl}_2\text{Ti}_3\text{O}_{10}$). Sample A shows more peaks compared to sample B with increasing heat treatment temperature. The number of peaks is higher than those reported in the previous work [5], which can be correlated with the MgO content of the glass. The MgO content used by Quyang et al. and Shao et al. [5] was higher than in this composition, which according to Amista et al. [26], lowers the temperature of crystallisation. Heat treatment at 1050 °C for 2 h induces crystallisation of $\text{Mg}_2\text{Al}_6\text{Ti}_7\text{O}_{25}$ (JCPDF card: 5-451) and magnesium aluminium oxide (M), MgAl_2O_4 (JCPDF card: 73-1959). The distinct peak at $26.14^\circ 2\theta$ indicated the presence of high quartz (β -QSS) solid solution with high intensity. The intensity of this reflection slightly increased when the temperature was increased to 1080 °C, and shifted to $26.46^\circ 2\theta$ corresponding to α -quartz solid solution (Q), SiO_2 (JCPDS card 81-65). The sample heat treated at 1100 °C indicates that the composition of magnesium aluminium titanate ($\text{Mg}_2\text{Al}_6\text{Ti}_7\text{O}_{25}$) is transforming to $\text{Mg}_{0.3}\text{Al}_{1.4}\text{Ti}_{1.3}\text{O}_5$, which corresponds to increased aluminium content and reduced magnesium and titanium contents as compared to the original T phase. In contrast with the previous studies [6], the little or no formation of magnesium aluminium silicate was observed.

After the heat treatment at 1140 °C (the onset of peak) the reflections due to magnesium aluminium titanate and

Fig. 3 XRD patterns of heat treated glass of $\text{MgO}-\text{Al}_2\text{O}_3-\text{SiO}_2$ samples, annealed at 700 °C (sample A) and 570 °C (sample B) prior to the heat treatment. T magnesium aluminium titanate, M magnesium aluminate, S magnesium silicate, A aluminium titanate, Q quartz



magnesium aluminium oxide disappeared and the glass phase was also minimised. Instead aluminium titanate (A), Al_2TiO_5 (JCPDS card 70-1435) and α -quartz solid solutions (α -QSS) along with a small amount of magnesium silicate (S), Mg_2SiO_4 (JCPDS card 34-556) was observed, likely to be due to the disappearance of glass.

Sample B

XRD results show a glassy phase with the high background level and significant XRD peaks were not observed after the heat treatment at the exothermic crystallisation peak of crystallisation.

Glass B4 treated at 950 °C shows two broad peaks at 37.29° and 65.94° 2θ corresponding to magnesium aluminium oxide (M) phase. This is significantly different result compared to sample A4 heat treated at the same temperature. Heat treatments at 1050 and 1080 °C led to the precipitation of magnesium aluminium titanate, $\text{T}(\text{Mg}_2\text{Al}_6\text{Ti}_7\text{O}_{25})$ and magnesium aluminium oxide (MgAl_2O_4). The XRD pattern of B6 heat treated at 1080 °C showed that the sharp peak at 26.09° 2θ shifted to 26.30° 2θ which can be attributed to a change in the magnesium aluminium titanate composition to $\text{Mg}_{0.3}\text{Al}_{1.4}\text{Ti}_{1.3}\text{O}_5$. Small peaks appeared when the temperature increased by 30 °C only. Increasing the temperature up to 1140 °C showed that magnesium aluminium titanate (A) and magnesium aluminium oxide phases remained, the glass phase was minimised and high quartz was also formed.

Physical and mechanical properties

Density increased with heat treatment temperatures from the amorphous glass phase towards the onset of the crystallisation temperatures for sample A, and slightly decreased at the onset of the second peak of crystallisation (Fig. 4). Density increased gradually from 1050 to 1140 °C. The average difference in density between 1050 and 1140 °C is approximately 8.8% for both samples. The density profile of both samples is similar between 950° to 1100° [5, 6, 19] with the highest value found after crystallisation at 1140 °C [6].

Figure 5 shows load-displacement curves for the original MAS glass and three glass ceramics produced in this study. As the heat treatment temperatures were increased, the depth of indentation decreased under the same load (Fig. 5) reflecting an increase in sample hardness. No significant differences were observed in the mechanical properties of the two different sample series (see Table 3). The influence of heat treatment temperature on the mechanical properties is shown in Figs. 6 (hardness) and 7 (reduced modulus).

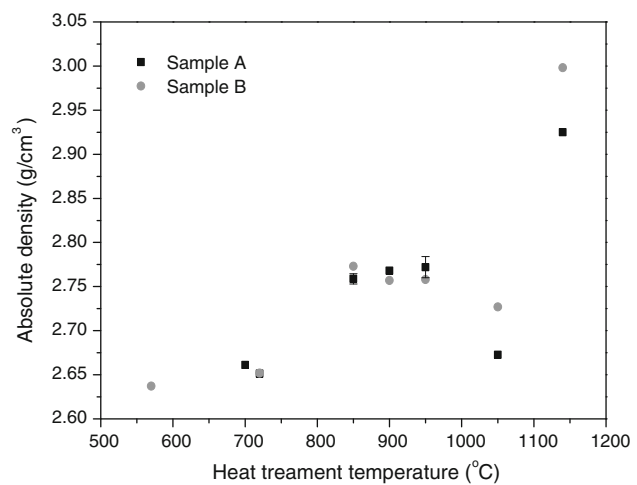


Fig. 4 Densities of the MAS samples at various heat treatment temperatures

Figures 6 and 7 show that the hardness and the reduced elastic moduli increase with the increased heat treatment temperature. These properties are improved compared to those of the parent glass [8] and especially hardness values of both systems are comparable with the literature [5, 6]. The overall properties are acceptable for high-temperature application where both samples show good mechanical properties.

Scanning electron microscopy (SEM)

From the SEM analysis presented in Fig. 8a–c for sample A, it can be seen that the increase in heat treatment temperatures had a notable influence on the microstructure and morphology of MAS glass-ceramic studied in this study. The heat treatments lead to the nucleation of crystals in glass, transforming the system in two phases, prominent droplet and glassy phases. The crystals observed at 950 °C are significantly larger than those depicted at 900 °C,

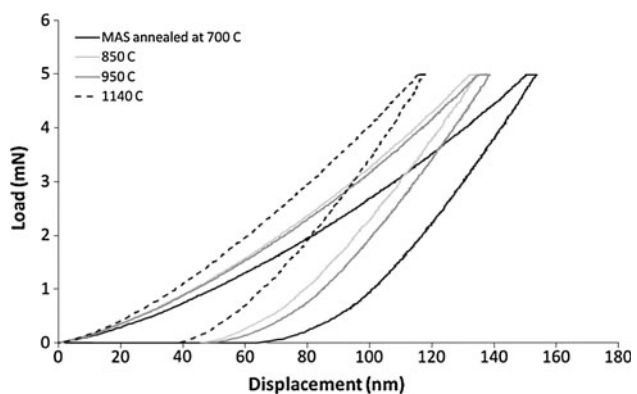
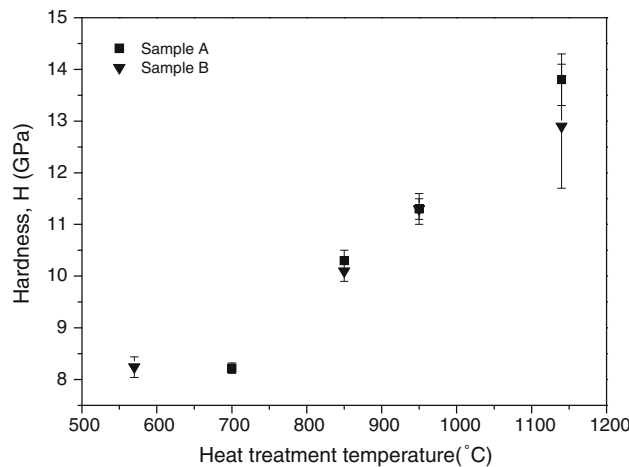
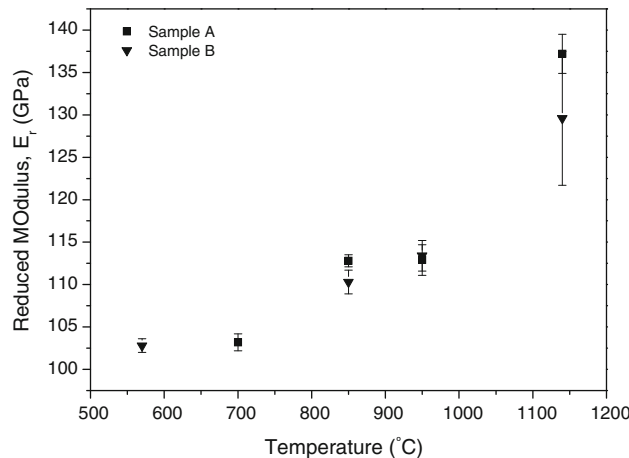


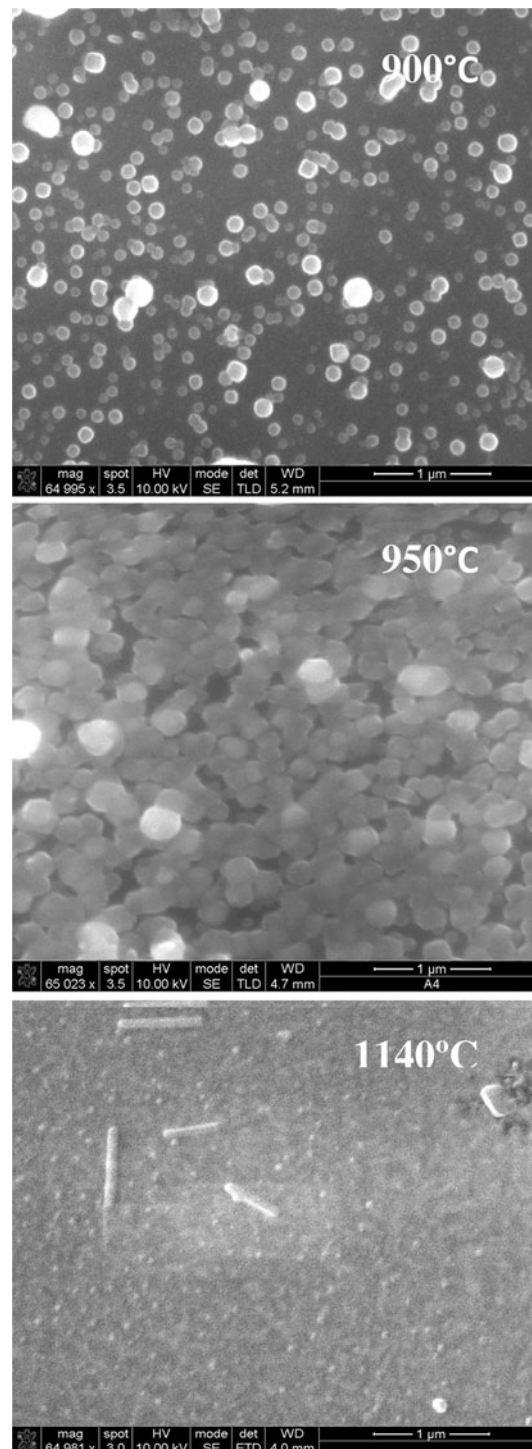
Fig. 5 Load-displacement curves for MAS glass annealed at 700 °C (sample A) and further subjected to different heat treatment temperatures (leading to formation of crystalline phases). The sample annealed at 570 °C showed a similar behaviour

Table 3 Reduced modulus and hardness results of the selected glasses, as measured by the nanoindentation technique

Temperature (°C)	Reduced modulus (GPa)		Hardness (GPa)	
	Sample A	Sample B	Sample A	Sample B
570	—	102.8 ± 0.8	—	8.24 ± 0.2
700	103.2 ± 1.0	—	8.22 ± 0.1	—
850	112.8 ± 0.7	110.3 ± 1.4	10.3 ± 0.2	10.1 ± 0.2
950	112.9 ± 1.8	113.4 ± 1.8	11.3 ± 0.2	11.3 ± 0.3
1140	137.2 ± 2.3	129.6 ± 7.9	13.8 ± 0.5	12.9 ± 1.2

**Fig. 6** Hardness results of MAS systems at various heat treatment regimes**Fig. 7** Reduced modulus values of MAS systems at various heat treatment regimes

indicating that an increase in the crystallisation temperature enhanced crystal growth. The droplet-shaped phase separation was initiated around 900 °C where MAT made its appearance, detected by XRD as shown in Fig. 3 (sample A). The morphology of MAS glass-ceramic scanned after the heat treatment at 950 °C showed that the crystal

**Fig. 8** SEM micrographs of the crystallised MgO-Al₂O₃-SiO₂ at **a** 900 °C, **b** 950 °C and **c** 1140 °C (sample A)

droplets (initiated at 900 °C) increased in quantity and size and formed numerous boundaries. A similar phenomenon was reported in a different system using the same nucleating agent by Shyu and Wu [27] and Minsheng et al. [28]. Figure 8c shows the morphology of the sample crystallised at 1140 °C, where the quantity of droplet-shaped crystals

increased, whilst decreasing in their sizes. A small number of crystals transformed into needle-like shapes.

Correlation between physical and mechanical properties in MAS

Figure 9a and b presents the correlations between the physical and mechanical properties of MAS glass-ceramics across the range of heat treatment temperatures used in this study. The nanohardness and the reduced modulus were found to be almost linearly correlated with the density and the type of crystalline phases [5].

Conclusion

The crystallisation behaviour of $\text{MgO}-\text{Al}_2\text{O}_3-\text{SiO}_2$ glass-ceramics nucleated with TiO_2 was investigated. The

temperature increase enhanced the rigidity of the glass structure, thereby superior and reliable properties such as density, nanohardness and reduced Young's modulus were successfully derived in the MAS system prepared at different annealing and subsequent heat treatment regimes. The thermo-mechanical properties were correlated to the crystalline phases present in the system. SEM analysis showed that there was a significant variation in morphology of the crystalline phases with the changes in the heat treatment temperatures.

Acknowledgements The authors wish to express their thanks to Mr Dean Haylock, Miss Bev Lane, Mr Philip Staton and Mr Pete Bailey for their technical assistance with glass melting, thermal analysis, sample preparation and technical advice. ZS would like to thank Universiti Teknikal Malaysia Melaka for granting her concession and study leave to undertake her PhD degree. The authors also wish to acknowledge Alstom (Areva) for the use of DTA.

References

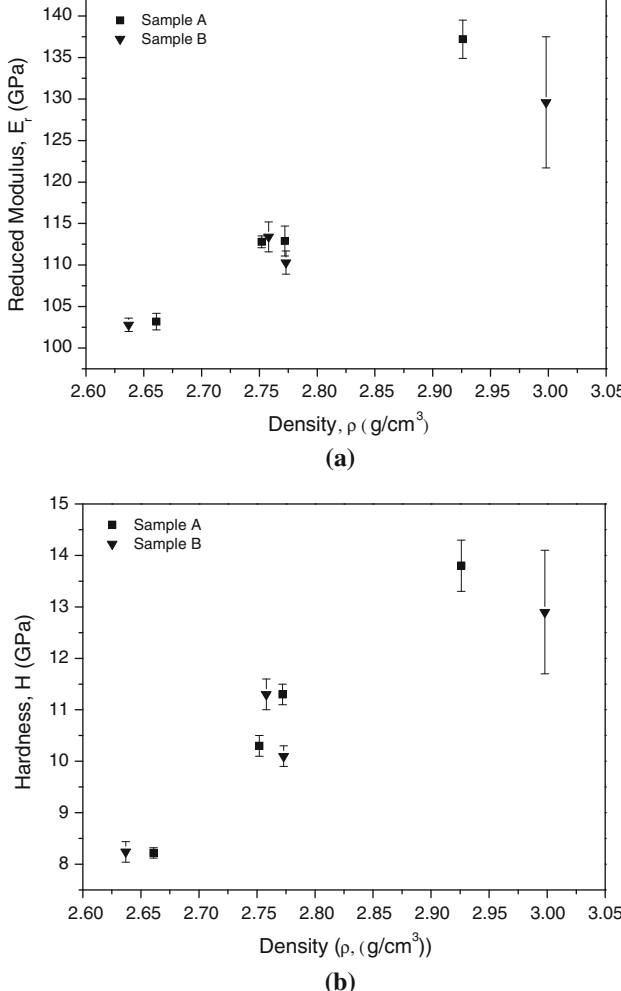


Fig. 9 Physical and mechanical properties of MAS sample A and B at different densities. **a** Reduced modulus, **b** hardness

1. Lawrence CW, Briggs GAD (1993) J Mater Sci 28:3645. doi: [10.1007/BF01159848](https://doi.org/10.1007/BF01159848)
2. Reich CH, Brückner R (1997) Compos Sci Technol 57:533
3. Yilmaz R, Taylor R (2007) J Mater Sci 42:4115. doi: [10.1007/s10853-007-1656-0](https://doi.org/10.1007/s10853-007-1656-0)
4. Ahn JM, Mall S (2009) Int J Appl Ceram Technol 6(1):45
5. Shao H, Liang K, Zhou F, Wang G, Hu A (2005) Mater Res Bull 40:499
6. Wange P, Höche T, Rüssel C, Schnapp JD (2002) J Non-Cryst Solids 298:137
7. Owate IO, Freer R (1990) J Mater Sci 25:5291. doi: [10.1007/BF00580163](https://doi.org/10.1007/BF00580163)
8. Gupta PK (1988) In: Bunsell AR (ed) Fibre reinforcements for composite materials. Elsevier, Amsterdam
9. McMillan PW (1979) Glass-ceramic. Academic, London
10. Strand Z (1986) Glass-ceramic materials. Elsevier, Amsterdam
11. Hwang SP, Wu JM (2001) J Am Ceram Soc 84:1108
12. Gregory AG, Veasay TJ (1973) J Mater Sci 8(3):324. doi: [10.1007/BF00550151](https://doi.org/10.1007/BF00550151)
13. Rawson H (1988) Properties and applications of glass. Elsevier, New York
14. Ashbee KHG (1973) J Mater Sci 10:911. doi: [10.1007/BF00823206](https://doi.org/10.1007/BF00823206)
15. Onishi M, Kyoto M, Watanabe M (1991) J Appl Phys 30(6A):988
16. Sakamoto A, Yamamoto S (2003) J Mater Sci 38:2305. doi: [10.1023/A:1023920110755](https://doi.org/10.1023/A:1023920110755)
17. Goswami M, Mirza T, Sarkar A, Manikandan S, Sangeeta SL, Verma KR, Gurumurthy VK, Shrikhande Kothiyal GP (2001) Bull Mater Sci 23(5):377
18. Halváč J (1983) The technology of glass and ceramic: an introduction. Elsevier, Amsterdam
19. Zdaniewski W (1973) J Mater Sci 8:192. doi: [10.1007/BF00550667](https://doi.org/10.1007/BF00550667)
20. Goel A, Shaaban ER, Melo FCL, Ribeiro MJ, Ferreira JMF (2007) J Non-Cryst Solids 353:2383
21. Shao H, Liang K, Peng F (2004) Ceram Int 30:927
22. Weaver DT, Van Aken DC, Smith JD (2004) J Mater Sci 39:51. doi: [10.1023/B:JMSC.0000007727.10682.b6](https://doi.org/10.1023/B:JMSC.0000007727.10682.b6)
23. Quyang XQ, Xiao ZH, Lu AX (2009) Adv Appl 108:178
24. Oliver WC, Pharr GM (1992) J Mater Res 7(6):1564

25. Doerner MF, Nix WD (1986) J Mater Res 1:601
26. Amista P, Cesari M, Montena A, Gnappi G, Lan L (1995) J Non-Cryst Solids 192&193:529
27. Shyu JJ, Wu JM (1991) J Mater Sci Lett 10:1056
28. Minsheng M, Wen N, Yali W, Zhongjie W, Fengmei L (2008) J Non-Cryst Solids 354:5395